

BRIEF COMMUNICATIONS

Ibuprofen-like activity in extra-virgin olive oil

Enzymes in an inflammation pathway are inhibited by oleocanthal, a component of olive oil.

Newly pressed extra-virgin olive oil contains oleocanthal — a compound whose pungency induces a strong stinging sensation in the throat, not unlike that caused by solutions of the non-steroidal anti-inflammatory drug ibuprofen¹. We show here that this similar perception seems to be an indicator of a shared pharmacological

activity, with oleocanthal acting as a natural anti-inflammatory compound that has a potency and profile strikingly similar to that of ibuprofen. Although structurally dissimilar, both these molecules inhibit the same cyclooxygenase enzymes in the prostaglandin-synthesis pathway.

The agent in extra-virgin olive oil responsible for throat irritation is thought to be the dialdehydic form of (–)deacetoxy-ligstroside aglycone² (or oleocanthal, with oleo- for olive, -canth- for sting, and -al for aldehyde) (Fig. 1). To confirm this, we isolated (–)oleocanthal from different premium olive oils and measured its intensity as a throat irritant. We found that irritation intensity was positively correlated with oleocanthal concentration. Although this finding indicates that oleocanthal is probably the principal irritating compound in olive oil, it was possible that

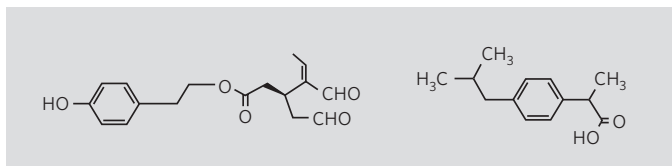


Figure 1 | Structures of (–)oleocanthal (left) and the anti-inflammatory drug ibuprofen (right). How they underpin the similar throat-irritating and pharmacological properties of the two compounds is unclear as yet.

co-elution of a minor component or a mixture of components could be causing the burning sensation². We therefore completed a *de novo* synthesis of oleocanthal, assigned the absolute stereochemistry (A.B.S. and Q.H., unpublished results), and tested the throat-irritant properties of this synthetic (–)oleocanthal, dissolved in non-irritating corn oil. The effect was comparable to that of premium extra-virgin olive-oil oleocanthal and was also dose-dependent. (For details and for methods, see supplementary information.)

Forty years ago, it was found that the bitterness of certain compounds correlated with their pharmacological activity³. On the basis of their shared irritant properties, we therefore tested whether oleocanthal might mimic the pharmacological effects of ibuprofen (Fig. 1), a potent modulator of inflammation and analgesia⁴. Ibuprofen is a non-selective

inhibitor of the cyclooxygenase enzymes COX-1 and COX-2, but not of lipoxygenase⁴, which catalyse steps in the biochemical inflammation pathways derived from arachidonic acid. We found that, like ibuprofen, both enantiomers of oleocanthal caused dose-dependent inhibition of COX-1 and COX-2 activities but

had no effect on lipoxygenase *in vitro* (Table 1).

Our findings raise the possibility that long-term consumption of oleocanthal may help to protect against some diseases by virtue of its ibuprofen-like COX-inhibiting activity^{5,6}. If 50 g of extra-virgin olive oil containing up to 200 µg per ml oleocanthal is ingested per day⁷, of which 60–90% is absorbed^{8,9}, then this corresponds to an intake of up to 9 mg per day. This dose is relatively low, corresponding to about 10% of the ibuprofen dosage recommended for adult pain relief, but it is known that regular low doses of aspirin, for example, another COX inhibitor, confer cardiovascular health benefits¹⁰. Ibuprofen is associated with a reduction in the risk of developing some cancers⁵ and of platelet aggregation in the blood¹¹, as well as with the COX-independent secretion of amyloid-β42 peptide in a mouse model of Alzheimer's disease⁶. A Mediterranean diet, which is rich in olive oil, is believed to confer various health benefits, some of which¹² seem to overlap with those attributed to non-steroidal anti-inflammatory drugs.

Our discovery of COX-inhibitory activity in a component of olive oil offers a possible mechanistic explanation for this link.

Gary K. Beauchamp*, **Russell S. J. Keast*†**, **Diane Morel‡**, **Jianming Lin§**, **Jana Pikaš**, **Qiang Han||**, **Chi-Ho Lee*†**, **Amos B. Smith*||**, **Paul A. S. Breslin***

*Monell Chemical Senses Center, †Department of Pharmacology and Toxicology, University of the Sciences in Philadelphia, and ||Department of Chemistry, University of Pennsylvania, Philadelphia, Pennsylvania 19104, USA
e-mail: breslin@monell.org

‡Present addresses: Food Science, RMIT University, Melbourne, Victoria 3001, Australia (R.S.J.K.); Animal Resources Research Center, Konkuk University, Gwangjin-Gu, Seoul 143-130, South Korea (C.-H.L.)

§ Firmenich, PO Box 5880, Princeton, New Jersey 08543, USA

Table 1 | Selective inhibition of COX enzymes by oleocanthal enantiomers

Agent	Concentration (µM)	COX-1 (%)	COX-2 (%)	15-LO (%)
(–)Oleocanthal	100	83.5 ± 3.5	70.9 ± 8.6	0.4 ± 0.8
	25	56.1 ± 3.2	56.6 ± 9.5	0.0 ± 0.0
	7	24.6 ± 7.3	14.5 ± 2.3	0.0 ± 0.0
(+)Oleocanthal	100	68.0 ± 15.2	69.6 ± 3.9	3.5 ± 5.5
	25	54.5 ± 4.6	41.3 ± 15.9	0.7 ± 1.0
	7	24.6 ± 7.5	6.1 ± 4.2	0.0 ± 0.0
Ibuprofen	25	17.8 ± 2.3	12.7 ± 3.6	0.2 ± 0.3
	7	0.0	1.3	ND
Indomethacin	25	90.1	89.8	0.1 ± 0.9
	7	86.6	66.3	0.5 ± 0.1
NDGA	25	ND	ND	63.1 ± 0.8
	7	ND	ND	52.5 ± 1.1
caffeic acid	25	ND	ND	25.2 ± 2.2
	7	ND	ND	19.8 ± 1.3

Percentage inhibition of cyclooxygenases 1 and 2 (COX-1, COX-2) and 15-lipoxygenase (15-LO) by three different concentrations of oleocanthal and of ibuprofen are presented as mean ± s.e.m. for three independent experiments. ND, not determined. Indomethacin was used as a positive (inhibitory) control in the cyclooxygenase assays and *nor*-dihydroguaiaretic acid (NDGA) and caffeic acid were used as positive (inhibitory) controls in the lipoxygenase assay. The concentrations for 50% inhibition (IC₅₀; calculated by least-squares regression analysis of inhibition versus concentration) for the natural (–) oleocanthal are 23 µM and 28 µM for COX-1 and COX-2, respectively; IC₅₀ values for (+) oleocanthal are 25 µM and 40 µM for COX-1 and COX-2, respectively; IC₅₀ values for ibuprofen are 5 µM and 223 µM for COX-1 and COX-2, respectively¹³. (For methods, see supplementary information.)

- Breslin, P. A. S., Gingerich, T. N. & Green, B. G. *Chem. Sens.* **26**, 55–66 (2001).
- Andrewes, P., Busch, J. L. H. C., De Joode, T., Groenewegen, A. & Alexandre, H. *J. Agric. Food Chem.* **51**, 1415–1420 (2003).
- Fischer, R., Griffen, F., Archer, R. C., Zinsmeister, S. C. & Jastram, P. S. *Nature* **207**, 1049–1053 (1965).
- Vane, J. R. & Botting, R. M. *Inflamm. Res.* **44**, 1–10 (1995).
- Harris, R. E., Beebe-Donk, J., Doss, H. & Burr Doss, D. *Oncol. Rep.* **13**, 559–583 (2005).
- Zhou, Y. *et al. Science* **302**, 1215–1217 (2003).
- Hu, F. N. *Engl. J. Med.* **348**, 2595–2596 (2003).
- Tuck, K., Freeman, M., Hayball, P., Stretch, G. & Stupans, I. *J. Nutr.* **131**, 1993–1996 (2001).
- Miro-Casas, E. *et al. Clin. Chem.* **49**, 945–952 (2003).
- Hennekens, C. H. *Am. J. Man. Care* **8** (suppl.), 691–700 (2002).
- Lefer, A. M., Muller, H. F. & Smith, J. B. *Br. J. Pharmacol.* **83**, 125–130 (1984).
- Togna, G. I., Togna, A. R., Franconi, M., Marra, C. & Guiso, M. *J. Nutr.* **133**, 2532–2536 (2003).
- Mitchell, J. A. *et al. Proc. Natl Acad. Sci. USA* **90**, 11693–11697 (1993).

Supplementary information accompanies this communication on *Nature's* website.
Competing financial interests: declared none.
 doi:10.1038/437045a

GEOPHYSICS

A moving fluid pulse in a fault zone

In the Gulf of Mexico, fault zones are linked with a complex and dynamic system of plumbing in the Earth's subsurface. Here we use time-lapse seismic-reflection imaging to reveal a pulse of fluid ascending rapidly inside one of these fault zones. Such intermittent fault 'burping' is likely to be an important factor in the migration of subsurface hydrocarbons.

Faults have a dual function in that they can act as both an impediment to and, at times, a preferential pathway for fluid flow. Both types of behaviour are invoked in the petroleum industry to explain how hydrocarbons move from the location at which they are generated (for example, by flowing along faults¹) into fault-bounded reservoirs where they become trapped (for example, by a lack of flow across faults²). Several lines of evidence from the South Eugene Island Block 330 field, offshore Louisiana, USA, indicate that faults cutting through sequences of Pliocene and Quaternary sands and shales have hosted significant vertical fluid flow over the past 250,000 years, continuing to the present day^{3–5}.

We present an additional set of data obtained from seismic reflection imaging that

indicates fast fluid movement (more than 100 metres per year) along growth faults. Previously, we have demonstrated that reflections from the fault planes appearing in seismic data from South Eugene Island Block 330 contain information about the distribution of fluid pressures across faults⁶.

The South Eugene Island field is an ideal location for this study. Multiple vintages of seismic-reflection surveys can be interpreted in the context of abundant fluid pressure, geochemical and other data. Normal faults transect the field at dips of about 50° southwest and separate upthrown sediments saturated by highly pressurized fluids from relatively less pressurized downthrown sediments (see supplementary information). The fault zones are typically at the same pressure as the upthrown sediments⁴. However, exceptionally pressurized fluid was encountered in one penetration of a growth fault, the B-fault, in the A10ST well^{3,4}. It was proposed that the isolated pocket of anomalously high fluid pressure in the A10ST well could represent a spatially limited pulse of anomalously pressured fluid⁴.

To test the idea of a moving fluid pulse, or fault burp, we isolated the fault-plane reflections from the B-fault

in images derived from seismic surveys taken in 1985 and 1992 and looked for indications of movement. In Fig. 1, we show reflectivity as a function of position on the fault plane for both sets of data. Patches of high reflectivity, or 'bright spots', are known to be associated with the presence of fluids⁷. The most striking pattern in the fault reflectivity maps is the northeast movement of the areas of highest reflectivity

between 1985 and 1992. This movement, in the updip direction, is to be expected for a fluid pulse ascending the B-fault. Also note the correlation between the area of highest reflectivity in 1992 and the location of the intersection with the A10ST well (Fig. 1b), where highly pressurized fluid in the fault was observed in 1993 (ref. 4).

From the reflectivity maps at the B-fault, we estimate the movement of the fluid pulse to be of the order of 1 km between 1985 and 1992. The observed movement of 1 km is significant compared with typical errors encountered in the processing of seismic data (see supplementary information). Movement of 1 km between 1985 and 1992 corresponds to an average pulse speed of about 140 m yr⁻¹. Such geologically fast fluid flow up a vertically permeable fault agrees with the dynamic-capacity model of fault-bounded reservoirs⁸ and is consistent with a nonlinear fluid-flow model involving pressure-dependent permeability⁹. These fault burps are key to the understanding of fluid-migration mechanisms and fault-zone rheology in the Earth's crust.

Matthew M. Haney*†, **Roel Snieder***,
Jon Sheiman‡, **Steven Losh**†§

*Center for Wave Phenomena and Department of Geophysics, Colorado School of Mines, Golden, Colorado 80401, USA

e-mail: mmhaney@sandia.gov

‡Shell International Exploration & Production, Houston, Texas 77025, USA

§Department of Earth and Atmospheric Sciences, Cornell University, Ithaca, New York 14853, USA

†Present addresses: Sandia National Laboratories, Geophysics Department, PO Box 5800 MS 0750, Albuquerque, New Mexico 87185-0750, USA (M.H.); Department of Chemistry and Geology, Minnesota State University, TN242, Mankato, Minnesota 56001, USA (S.L.).

- Hooper, E. C. D. *J. Petrol. Geol.* **14**, 161–180 (1991).
- Holland, D. S., Leedy, J. B. & Lammlein, D. R. in *Structural Traps III, Tectonic Fold and Fault Traps: AAPG Treatise of Petroleum Geology Atlas of Oil and Gas Fields* (eds Beaumont, E. A. & Foster, N. H.) 103–143 (AAPG, Tulsa, 1990).
- Anderson, R. N., He, W., Hobart, M. A., Wilkinson, C. R. & Roice, H. R. *The Leading Edge* **10**, 12–17 (1991).
- Losh, S., Eglinton, L., Schoell, M. & Wood, J. *AAPG Bull.* **83**, 244–276 (1999).
- Whelan, J. K., Eglinton, L., Kennicutt, M. C. II & Qian, Y. *Geochim. Cosmochim. Acta* **65**, 3529–3555 (2001).
- Haney, M. *et al. in Proc. EAGE Spec. Sess. Fault and Top Seals* (eds Engelder, T., Konstanty, J. & Grauls, D.) 0–7 (EAGE, Houten, 2004).
- Dobrin, M. B. *Introduction to Geophysical Prospecting* (McGraw-Hill, New York, 1976).
- Finkbeiner, T., Zoback, M. D., Stump, B. & Flemings, P. *AAPG Bull.* **85**, 1007–1031 (2001).
- Rice, J. R. in *Fault Mechanics and Transport Properties of Rocks* (eds Evans, B. & Wong, T.-F.) 475–503 (Academic, San Diego, 1992).

Supplementary information accompanies this communication on *Nature's* website.

Competing financial interests: declared none.
 doi:10.1038/437046a

BRIEF COMMUNICATIONS ARISING online
 ▶ www.nature.com/bca see *Nature* contents.

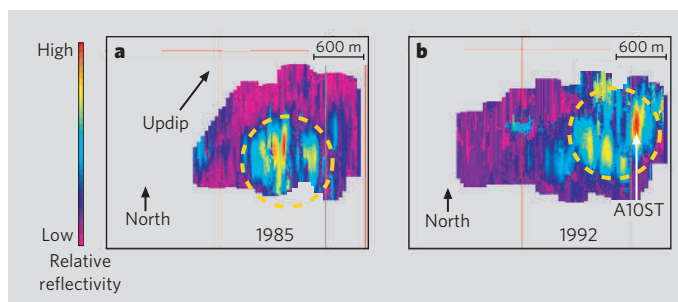


Figure 1 | A fault caught in the act of burping. **a**, Map of the B-fault showing reflectivity from the fault plane in 1985. The area of highest reflectivity is circled in gold. **b**, Map of the B-fault reflectivity, as shown in **a**, but from 1992. The data extend over a slightly larger area than in **a**; however, the spatial perspective is identical. The area of highest reflectivity, circled in gold, is shifted roughly 1 km north-east in the updip direction relative to its location in 1985, as would be expected for a fluid pulse ascending the B-fault; this movement is depicted by the arrow in **a**. Also shown is the location of the A10ST well intersection, where exceptionally high fluid pressures were encountered while drilling into the B-fault zone in 1993.